

2008

Superconductivity close to magnetic instability in $\text{Fe}(\text{Se}_{1-x}\text{Te}_x)_{0.82}$

M H. Fang

H M. Pham
University of New Orleans

B Qian

T J. Liu

E K. Vehstedt

See next page for additional authors

Follow this and additional works at: https://scholarworks.uno.edu/phys_facpubs



Part of the [Physics Commons](#)

Recommended Citation

Phys. Rev. B 78, 224503 (2008)

This Article is brought to you for free and open access by the Department of Physics at ScholarWorks@UNO. It has been accepted for inclusion in Physics Faculty Publications by an authorized administrator of ScholarWorks@UNO. For more information, please contact scholarworks@uno.edu.

Authors

M H. Fang, H M. Pham, B Qian, T J. Liu, E K. Vehstedt, Y Liu, L Spinu, and Z Q. Mao



Superconductivity close to magnetic instability in $\text{Fe}(\text{Se}_{1-x}\text{Te}_x)_{0.82}$

M. H. Fang,¹ H. M. Pham,² B. Qian,¹ T. J. Liu,¹ E. K. Vehstedt,¹ Y. Liu,³ L. Spinu,² and Z. Q. Mao¹

¹*Department of Physics, Tulane University, New Orleans, Louisiana 70118, USA*

²*Department of Physics and Advanced Materials Research Institute, University of New Orleans, New Orleans, Louisiana 70148, USA*

³*Department of Physics, The Pennsylvania State University, University Park, Pennsylvania 16801, USA*

(Received 15 October 2008; revised manuscript received 9 November 2008; published 3 December 2008)

We report our study of the evolution of superconductivity and the phase diagram of the ternary $\text{Fe}(\text{Se}_{1-x}\text{Te}_x)_{0.82}$ ($0 \leq x \leq 1.0$) system. We discovered a superconducting phase with $T_{c,\text{max}}=14$ K in the $0.3 < x < 1.0$ range. This superconducting phase is suppressed when the sample composition approaches the end member $\text{FeTe}_{0.82}$, which exhibits an incommensurate antiferromagnetic order. We discuss the relationship between the superconductivity and magnetism of this material system in terms of recent results from neutron-scattering measurements. Our results and analyses suggest that superconductivity in this class of Fe-based compounds is associated with magnetic fluctuations and therefore may be unconventional in nature.

DOI: [10.1103/PhysRevB.78.224503](https://doi.org/10.1103/PhysRevB.78.224503)

PACS number(s): 74.70.-b, 74.25.Dw, 74.25.Fy

I. INTRODUCTION

The discovery of high-temperature superconductivity up to 56 K in the iron arsenide compounds $\text{LnFeAsO}_{1-x}\text{F}_x$ (Ln = lanthanides) (Refs. 1–6) is quite surprising since iron ions in many compounds have magnetic moments and they normally form an ordered magnetic state. Neutron-scattering investigations of these materials have demonstrated that there exists a long-range spin-density wave (SDW)-type antiferromagnetic order in the undoped parent compound LaFeAsO .^{7,8} This suggests that magnetic fluctuations may play an essential role in mediating superconducting pairing in doped materials^{9–11} similar to the scenario seen in high- T_c cuprates. The newly discovered binary superconductor FeSe ($T_c \approx 10$ K) is another example of an iron-based superconductor.¹² Interestingly, this binary system contains antiferromagnetic planes which are isostructural to the FeAs layer found in the quaternary iron arsenide.¹³ The T_c of this material was increased to 27 K by applying hydrostatic pressure,¹⁴ suggesting that the simple binary FeSe may possess some essential ingredients for achieving high-temperature superconductivity in FeAs-based compounds. Band-structure calculations show that the Fermi-surface structure of FeSe is indeed very similar to that of the FeAs-based compounds.¹⁵

FeSe has a complicated phase diagram originating from nonstoichiometric compositions.¹⁶ The structure and magnetic properties of this system depend sensitively on the relative ratio of Se:Fe. For example, $\text{FeSe}_{0.82}$ has a PbO-type structure with a tetragonal space group $P4/nmm$ and is superconducting, while $\text{FeSe}_{1.14}$ has a hexagonal structure and is a ferrimagnet.¹⁶ In order to determine if the superconductivity in FeSe is associated with magnetism, the magnetic properties of other related iron chalcogen binary compounds possessing a layered tetragonal structure similar to FeSe should be examined. We note that in the FeTe binary system the composition in the $\text{FeTe}_{0.85}$ - $\text{FeTe}_{0.95}$ range is tetragonal, isostructural to the $\text{FeSe}_{0.82}$ superconductor,¹² and ferrimagnetic.¹⁷ Given that $\text{FeSe}_{0.82}$ is superconducting, it is particularly interesting to investigate how the superconducting state evolves toward a magnetically ordered state with Te

substitution for Se. For this purpose, we prepared polycrystalline samples of the $\text{Fe}(\text{Se}_{1-x}\text{Te}_x)_{0.82}$ ($0 \leq x \leq 1.0$) series and characterized their electronic and magnetic properties. We discovered two different superconducting phases, one for $0 \leq x < 0.15$ and the other for $0.3 < x < 1.0$, and the coexistence of the two phases for $0.15 \leq x \leq 0.3$. The $0.3 < x < 1.0$ phase has the highest superconducting transition temperature of $T_{c,\text{max}}=14$ K under ambient pressure. Most importantly, we found that this superconducting phase is suppressed only when the sample composition approaches the end member $\text{FeTe}_{0.82}$, which has a long-range magnetic order. These findings strongly suggest that superconductivity in Fe-based compounds is associated with magnetic fluctuations and therefore may be unconventional in nature.

II. EXPERIMENT

Our samples with nominal compositions $\text{Fe}(\text{Se}_{1-x}\text{Te}_x)_{0.82}$ ($x=0, 0.05, 0.2, 0.25, 0.3, 0.4, 0.5, 0.6, 0.7, 0.8, 0.9, \text{ and } 1.0$) were prepared using a solid-state reaction method. The mixed powder was first pressed into pellets, then sealed in an evacuated quartz tube and sintered at 700 °C for 24 h. The sample was then reground, pressed into pellets, and sintered again at 700 °C for 24 h. Structural characterization of these samples was performed using x-ray diffractometry and their compositions were analyzed using energy dispersive x-ray spectroscopy (EDXS).

Resistivity measurements were performed using a standard four-probe method in a physical property measurement system [(PPMS) Quantum Design]. The magnetization was measured using a superconducting quantum interference device (SQUID) (Quantum Design). Hall effects for the samples with $x=0.6$ and 1.0 were measured using a conventional four-probe method; the longitudinal resistivity component was eliminated by reversing the field direction.

III. RESULTS AND DISCUSSIONS

X-ray diffraction analyses showed all of our samples to be of high purity. Only a negligible amount of impurity phase β - FeSe was observed in the samples near the Se side. Figure

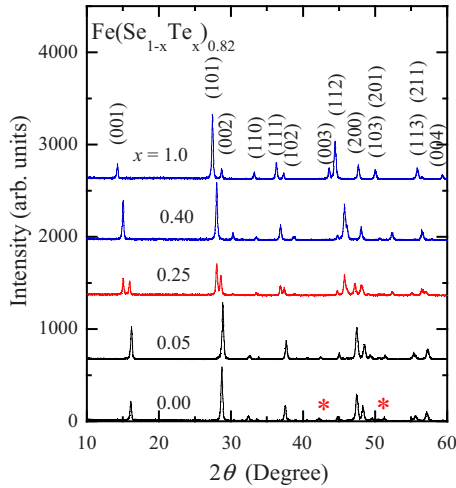


FIG. 1. (Color online) X-ray diffraction patterns of typical compositions in the $\text{Fe}(\text{Se}_{1-x}\text{Te}_x)_{0.82}$ series. Two different structural phases are observed in different composition ranges. $0 \leq x < 0.15$: phase A; $0.3 < x \leq 1$: phase B. Phases A and B coexist in the $0.15 < x < 0.3$ range where the diffraction peaks split into two sets. While phases A and B have the same tetragonal space group $P4/nmm$, they have remarkably different lattice parameters [see Fig. 2(a)]. Peaks marked by * for the $x=0$ sample: impurity phase (β -FeSe).

1 shows x-ray diffraction patterns of typical compositions. We find that the diffraction peaks of both end members $\text{FeSe}_{0.82}$ and $\text{FeTe}_{0.82}$ can be indexed with the tetragonal lattice $P4/nmm$, which is consistent with previously reported results,^{12,17} but their lattice parameters are remarkably different from each other, as shown in Fig. 2(a). Diffraction peaks exhibit systematic shifts with the variation in the Se:Te ratio either for $x > 0.3$ or $x < 0.15$. For $0.15 < x < 0.3$, however, all diffraction peaks split into two sets, implying a coexistence of two structural phases (e.g., the data of the $x=0.25$ sample in Fig. 1). This observation suggests that the structure of $\text{FeTe}_{0.82}$ is essentially different from that of $\text{FeSe}_{0.82}$ even though both of them can be described by a similar tetragonal lattice. Here we use A and B to denote these two structural phases, respectively. Structure A is stable for $0 \leq x < 0.15$, while structure B is stable for $0.3 < x \leq 1.0$. Both structural phases coexist within the $0.15 < x < 0.3$ range. The systematic variation in lattice parameters with x is presented in Fig. 2(a) for both structural phases. A clear transition between phases A and B can be identified in both the a and c lattice parameters near $x \sim 0.2$. For phase A, both a and c change only slightly with increasing x ; while for phase B, a and c increase more remarkably with increasing x .

Our EDXS analyses show that the sample composition slightly deviates from the nominal composition for samples composed of either phase A or phase B. For example, for the nominal composition $\text{Fe}(\text{Se}_{0.4}\text{Te}_{0.6})_{0.82}$, the measured average composition by EDXS is $\text{Fe}(\text{Se}_{0.40}\text{Te}_{0.62})_{0.88}$. The difference between them is within the limits of error for EDX analysis, suggesting that the actual composition of our samples is close to the nominal composition. This is also evidenced by the fact that most of the samples do not show any impurity phases.

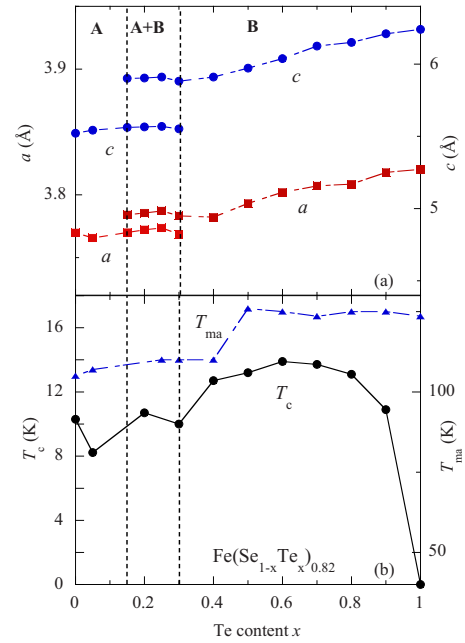


FIG. 2. (Color online) Lattice parameters (a), magnetic anomaly temperature T_{ma} , and the onset superconducting transition temperature T_c (b) as a function of Te content x in the $\text{Fe}(\text{Se}_{1-x}\text{Te}_x)_{0.82}$ series. The definitions of T_{ma} and T_c are shown in Figs. 3 and 4, respectively.

Phases A and B exhibit distinctly different electronic and magnetic properties. As shown in Figs. 2(b) and 3(a), phase A exhibits superconductivity with $T_c \sim 8\text{--}10$ K consistent with the reported superconductivity in $\text{FeSe}_{0.82}$.¹² Phase B, however, exhibits enhanced superconductivity with a maximum T_c of ~ 14 K. Both phases have resistivity ρ higher than that expected for metals (whose resistivity is usually < 1 m Ω cm) at their normal states; but they display different temperature dependences. Phase A shows a metallic behavior from room temperature to the superconducting transition temperature (e.g., the data of the $x=0, 0.2$ samples in Fig. 3). Phase B, however, shows a weak upturn before the superconducting transition. For samples with $0.2 < x < 0.6$, metallic temperature dependences occur at high temperatures, thus resulting in minima at low temperatures. The T_c of phase B varies with x with the maximum ($T_c=14$ K) occurring near $x \sim 0.6$. Phase B exhibits the superconducting state through $x \approx 0.9$, but it disappears in the $x=1.0$ end member. The difference between the superconducting states of phases A and B is also confirmed by magnetization measurements, as shown in Fig. 4(b).

In the nonsuperconducting $x=1.0$ sample $\text{FeTe}_{0.82}$, we observed two anomalies in the magnetic susceptibility χ , as denoted by the arrows in Fig. 4(a). One occurs near 125 K, below which $\chi(T)$ exhibits a striking irreversibility between field cooling (FC) and zero-field cooling (ZFC) histories [see Fig. 4(b)]; the other appears near 65 K where an anomalous peak in $\rho(T)$ is observed. The 125 K anomaly also occurs in all samples with $x > 0.4$ and this anomaly shifts down to 105–110 K when x is reduced below 0.4, as shown in Figs. 4(b) and 2(b) where the variation in the anomaly temperature T_{ma} with x is presented. The 65 K anomaly seen in $\text{FeTe}_{0.82}$,

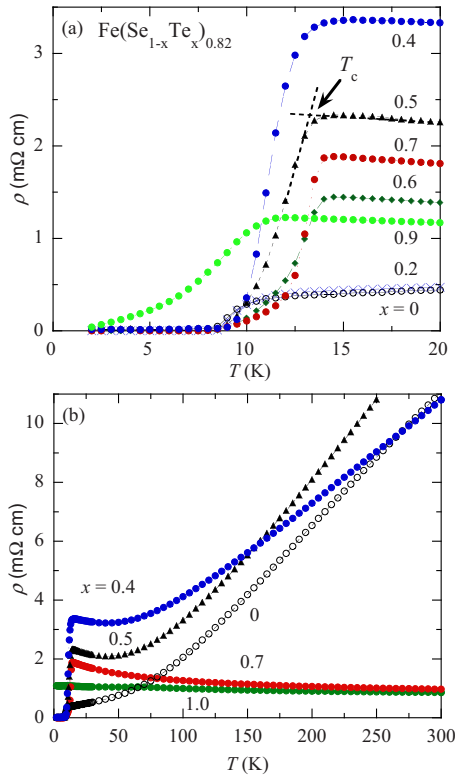


FIG. 3. (Color online) Resistivity as a function of temperature $\rho(T)$ for the samples with various Te content x . (a) $\rho(T)$ of the samples with typical compositions for $T < 20$ K. The superconducting onset transition temperature T_c is defined as the intersection between the linear extrapolations of the normal state $\rho(T)$ and the middle transition, as shown in the figure. (b) $\rho(T)$ of the samples with typical compositions in the 2–300 K range.

however, does not occur in any samples with $x < 1.0$.

Recent neutron-scattering measurements performed by Bao *et al.*¹³ using our samples show that the 65 K anomaly in $FeTe_{0.82}$ corresponds to simultaneous structural and antiferromagnetic transitions rather than the aforementioned ferromagnetic transition.¹⁷ The structure belongs to a tetragonal lattice with the space group $P4/nmm$ at high temperatures but distorts to a $Pmmn$ orthorhombic structure below 65 K. An incommensurate antiferromagnetic order, which includes both linear and spiral components, occurs below this structure transition temperature; this magnetic order propagates along the diagonal direction of the Fe square sublattice. Such a complex magnetic behavior is different from what was observed in the parent compound of FeAs-based superconductors where the antiferromagnetic order is commensurate and propagates along one edge of the Fe square sublattice.^{7,8}

In addition to the antiferromagnetic transition, this structure transition also results in an anomaly in the Hall coefficient. Our Hall-effect measurements were performed by sweeping the magnetic field at fixed temperatures. The transverse Hall resistance ρ_H exhibits a linear field dependence for each temperature. Figure 5 shows the Hall coefficient R_H as a function of temperature derived from the slope of $\rho_H(H)$. We find that R_H is negative and is hardly temperature dependent for $T > 65$ K, but it shows a remarkable upturn below 65 K. These observations indicate that charge carriers in

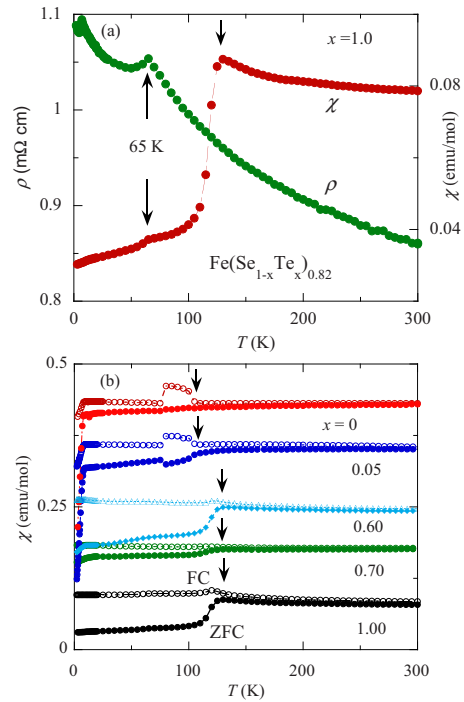


FIG. 4. (Color online) (a) Magnetic susceptibility χ and resistivity ρ as a function of temperature for the sample with $x=1.0$. An anomaly near 65 K is observed in both measurements. The arrow near 125 K indicates the magnetic anomaly temperature, below which χ exhibits marked irreversibility between FC and ZFC cooling histories as shown in panel (b). (b) Magnetic susceptibility $\chi(T)$ measured following FC and ZFC cooling histories for the samples with $x=0, 0.05, 0.6, 0.7$, and 1.0 . The transitions at low temperatures correspond to the superconducting Meissner effect. The Meissner effect is observed in all samples except for $x=1.0$.

$FeTe_{0.82}$ are mainly electrons and that the structure transition may lead to the change in electronic band structure and/or the variation in the scattering rate of charge carriers.

Regarding the magnetic anomaly near 125 K in $FeTe_{0.82}$, neutron-scattering measurements did not reveal any evidence of either structure or magnetic transition.¹⁸ Similar situations

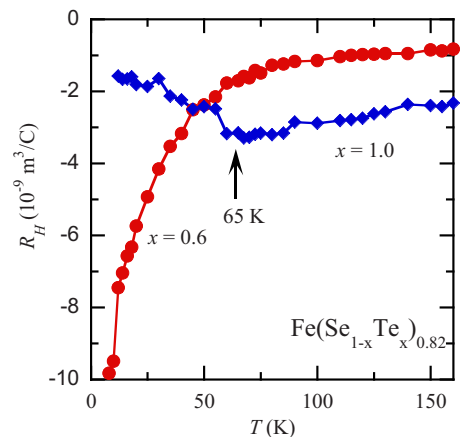


FIG. 5. (Color online) Hall coefficient as a function of temperature for $Fe(Se_{1-x}Te_x)_{0.82}$ with $x=0.6$ and 1.0 . The arrow indicates the structure transition temperature for the $x=1.0$ sample.

occur for other samples showing the 125 K magnetic anomaly (see below). However, we note that the magnetic anomaly at 105 K in $\text{FeSe}_{0.88}$ is associated with a tetragonal-triclinic structure transformation,¹² and a tetragonal-orthorhombic structural transformation at 70 K was also reported for a slightly different composition $\text{FeSe}_{0.92}$.¹⁹ Both results were obtained by high-resolution synchrotron x-ray diffraction measurements. Similar measurement is clearly necessary to clarify the origin of the magnetic anomalies observed in our samples.

Superconductivity in the Se-substituted samples appears to be related to the antiferromagnetic order in the end member $\text{FeTe}_{0.82}$. Neutron-scattering measurements have been performed on the $x=0.6$ sample which has the optimal $T_{c,\text{max}}=14$ K. Neither long-range magnetic order nor structural transition was observed in this sample though it shows the 125 K magnetic anomaly in susceptibility [see Fig. 4(b)]. Nevertheless short-range magnetic correlations at an incommensurate wave vector survive and the magnetic correlation length is about 4 Å.¹³ These short-range magnetic correlations depend on temperature; they start to occur below 75 K and enhance more rapidly below 40 K. Interestingly, we observed an anomalous temperature dependence in the Hall coefficient in the same temperature range for this sample. As seen in Fig. 5, the Hall coefficient R_H for the $x=0.6$ sample starts to drop below 75 K and a remarkable decrease occurs below 40 K consistent with the temperature dependence of the short-range magnetic order. These observations suggest strong interplay between spin and charge degrees of freedom in this material system and that the superconducting state is extremely close to an antiferromagnetic instability. Therefore the superconductivity in the $\text{Fe}(\text{Se}_{1-x}\text{Te}_x)_{0.82}$ should be associated with magnetic fluctuations and unconventional in nature similar to other FeAs-based superconductors.¹⁻⁸ In fact, evidence for unconventional superconductivity has been observed in recent NMR measurements for FeSe .²⁰

The band tuning is the most likely explanation for the presence of superconductivity in the Se-substituted samples. Since Te^{2-} and Se^{2-} have the same valence but different ionic radii, Te^{2-} substitution for Se^{2-} does not directly lead to charge-carrier doping but results in the variation in band structure which in turn may change the Fermi surface. Our Hall-effect measurement results shown in Fig. 5 reflect such changes.

Finally we would like to point out that the incommensurate antiferromagnetic structure of $\text{FeTe}_{0.82}$ discussed above differs from the previously reported magnetic structure of iron telluride $\text{FeTe}_{0.90}$, which was identified as a ferromagnet for high temperatures and a ferrimagnet below 63 K.¹⁷ For comparison, we also prepared a sample with the nominal composition $\text{FeTe}_{0.90}$ using the same solid-state reaction method stated above. Neutron-scattering measurements on this sample show that it is truly different from $\text{FeTe}_{0.82}$ in both crystal and magnetic structures.¹³ The structure transition temperature in $\text{FeTe}_{0.90}$ is shifted up to 75 K and the structure distorts to a monoclinic lattice below the transition rather than an orthorhombic lattice as in $\text{FeTe}_{0.82}$. The antiferromagnetic order, which occurs below the structural transition, becomes commensurate, in contrast with the incommensurate antiferromagnetic order in $\text{FeTe}_{0.82}$. As noted

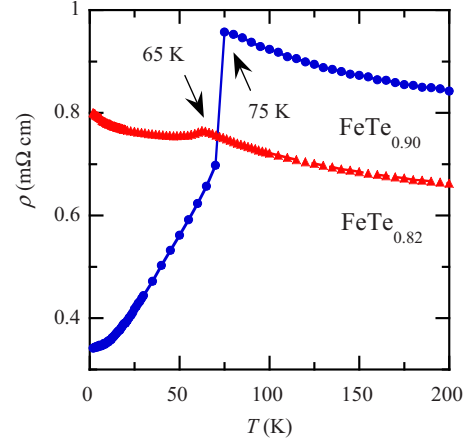


FIG. 6. (Color online) Resistivity as a function of temperature for $\text{FeTe}_{0.82}$ and $\text{FeTe}_{0.90}$. The arrows indicate the structure transition temperature for each sample.

above, the incommensurate antiferromagnetic state in $\text{FeTe}_{0.82}$ shows a nonmetallic temperature dependence in resistivity, while in $\text{FeTe}_{0.90}$ the commensurate antiferromagnetic state is accompanied by metallic transport properties as shown in Fig. 6. These results are inconsistent with those reported results in Ref. 17 for $\text{FeTe}_{0.90}$. One possible reason for this difference is that while our sample and the sample used in Ref. 17 have the same nominal composition, their actual phase might be somewhat different since the iron telluride system has a very complicated phase diagram and the preparation conditions between our samples and the samples used in Ref. 17 are very different, which may result in subtle structural changes.

IV. CONCLUSIONS

In summary, we report the evolution of superconductivity, magnetism, and structural transition in $\text{Fe}(\text{Se}_{1-x}\text{Te}_x)_{0.82}$ ($0 \leq x \leq 1$). The entire range of x was found to be superconducting except for the $x=1.0$ end member. Two different superconducting phases, coming from two tetragonal structures with the same space group and different lattice parameters, were identified: one for $0 \leq x < 0.15$ and the other for $0.3 < x < 1.0$. In the $0.15 \leq x \leq 0.3$ range, they were found to coexist. The maximum $T_c=14$ K occurs near $x=0.6$. In terms of the results from neutron-scattering studies, the superconductivity of this system seems intimately related with magnetic correlations. The nonsuperconducting end member $\text{FeTe}_{0.82}$ shows an incommensurate antiferromagnetic order; while in the Se-substituted superconducting samples, the long-range magnetic order evolves into short-range magnetic correlations. These short-range correlations enhance significantly as the temperature is decreased below 40 K and they lead to an anomalous temperature dependence in the Hall coefficient. These results strongly suggest that the superconductivity in this material system may be mediated by magnetic fluctuations and therefore unconventional in nature.

ACKNOWLEDGMENTS

The work at Tulane is supported by the NSF under Grant No. DMR-0645305, the DOE under Grant No. DE-FG02-07ER46358, the DOD ARO under Grant No. W911NF-08-

C-0131, and the Research Corporation. Work at UNO is supported by DARPA through Grant No. HR0011-07-1-0031. Work at Penn State is supported by the DOE under Grant No. DE-FG02-04ER46159 and DOD ARO under Grant No. W911NF-07-1-0182.

-
- ¹Y. Kamihara, T. Watanabe, M. Hirano, and H. Hosono, *J. Am. Chem. Soc.* **130**, 3296 (2008).
- ²X. H. Chen, T. Wu, G. Wu, R. H. Liu, H. Chen, and D. F. Fang, *Nature (London)* **453**, 761 (2008).
- ³G. F. Chen, Z. Li, D. Wu, G. Li, W. Z. Hu, J. Dong, P. Zheng, J. L. Luo, and N. L. Wang, *Phys. Rev. Lett.* **100**, 247002 (2008).
- ⁴H. H. Wen, G. Mu, L. Fang, H. Yang, and X. Zhu, *Europhys. Lett.* **82**, 17009 (2008).
- ⁵W. Lu, J. Yang, X. L. Dong, Z. A. Ren, G. C. Che, and Z. X. Zhao, *New J. Phys.* **10**, 063026 (2008).
- ⁶L.-J. Li, Y.-K. Li, Z. Ren, Y.-K. Luo, X. Lin, M. He, Q. Tao, Z.-W. Zhu, G.-H. Cao, and Z.-A. Xu, *Phys. Rev. B* **78**, 132506 (2008).
- ⁷C. de la Cruz, Q. Huang, J. W. Lynn, J. Li, W. Ratcliff II, J. L. Zarestky, H. A. Mook, G. F. Chen, J. L. Luo, N. L. Wang, and P. Dai, *Nature (London)* **453**, 899 (2008).
- ⁸A. S. Sefat, A. Huq, M. A. McGuire, R. Jin, B. C. Sales, D. Mandrus, L. M. D. Cranswick, P. W. Stephens, and K. H. Stone, *Phys. Rev. B* **78**, 104505 (2008).
- ⁹I. I. Mazin, D. J. Singh, M. D. Johannes, and M. H. Du, *Phys. Rev. Lett.* **101**, 057003 (2008).
- ¹⁰J. Dong, H. J. Zhang, G. Xu, Z. Li, G. Li, W. Z. Hu, D. Wu, G. F. Chen, X. Dai, J. L. Luo, Z. Fang, and N. L. Wang, *Europhys. Lett.* **83**, 27006 (2008).
- ¹¹G. Xu, W. M. Ming, Y. G. Yao, X. Dai, S. C. Zhang, and Z. Fang, *Europhys. Lett.* **82**, 67002 (2008).
- ¹²F.-C. Hsu, J.-Y. Luo, K.-W. Yeh, T.-K. Chen, T.-W. Huang, P. M. Wu, Y.-C. Lee, Y.-L. Huang, Y.-Y. Chu, D.-C. Yan, and M.-K. Wu, *Proc. Natl. Acad. Sci. U.S.A.* **105**, 14262 (2008).
- ¹³W. Bao, Y. Qiu, Q. Huang, M. A. Green, P. Zajdel, M. R. Fitzsimmons, M. Zhernenkov, M. H. Fang, B. Qian, E. K. Vehstedt, J. H. Yang, H. M. Pham, L. Spinu, and Z. Q. Mao, arXiv:0809.2058 (unpublished).
- ¹⁴Y. Mizuguchi, F. Tomioka, S. Tsuda, T. Yamaguchi, and Y. Takano, *Appl. Phys. Lett.* **93**, 152505 (2008).
- ¹⁵A. Subedi, L. Zhang, D. J. Singh, and M. H. Du, *Phys. Rev. B* **78**, 134514 (2008).
- ¹⁶W. Schuster, H. Mikler, and K. L. Komarek, *Monatsh. Chem.* **110**, 1153 (1979).
- ¹⁷J. Leciejewicz, *Acta Chem. Scand.* (1947-1973) **17**, 2593 (1963).
- ¹⁸W. Bao (private communication).
- ¹⁹S. Margadonna, Y. Takabayashi, M. T. McDonald, K. Kasperkiewicz, Y. Mizuguchi, Y. Takano, A. N. Fitch, E. Suard, and K. Prassides, *Chem. Commun. (Cambridge)* **2008**, 5607.
- ²⁰H. Kotegawa, S. Masaki, Y. Awai, H. Tou, Y. Mizuguchi, and Y. Takano, *J. Phys. Soc. Jpn.* **77**, 113703 (2008).